# Harnessing Machine Learning Models for Pavement Texture Clustering

Masud Rana Munna * and Kaustav Chatterjee

Posted Date: 17 March 2026

doi: 10.20944/preprints202603.1280.v1

Keywords: mean profile depth; gaussian mixture model; random forest model; centroid-based optimization; long-term pavement performance; machine learning model

 doi:10.20944/preprints202603.1280.v1



*Article*

# Harnessing Machine Learning Models for Pavement Texture Clustering

**Masud Rana Munna * and Kaustav Chatterjee**

PhD, School of Civil and Environmental Engineering, Oklahoma State University, Stillwater, OK 74078, USA

* Correspondence: mmunna@okstate.edu

**Abstract**

Pavement texture is a critical element affecting road safety and ride quality. It is affected by traffic volume, climate conditions, aggregate properties, and asphalt volumetric properties. This research aims to study the effect of different parameters on pavement texture using statistical and machine learning models. Pavement profile data and multiple variables affecting texture were collected from 192 SPS sections from the Long-Term Pavement Performance (LTPP) database. After data collection, pavement texture data were obtained from the pavement profile using ProVAL software and Python. Thereafter, the pavement texture was clustered into four diverse groups using the Gaussian Mixture Model (GMM), and the research determined cluster-specific profiles by applying centroid-based optimization techniques. Finally, an ordered logistic regression model and different machine learning models using K-nearest neighbor, random forest, extra trees, extreme gradient boosting, cat boosting, neural network, and weighted ensemble algorithm were developed to explore the parameters affecting the texture at diverse levels. The important parameters obtained from the statistical model were International Roughness Index (IRI), Annual Average Daily Truck Traffic (AADTT), temperature, and untreated subgrade, and from machine learning models were precipitation, IRI, AADTT, and 18-kips ESAL. Overall, this study significantly contributed to advancing the understanding and application of diverse impactful factors for pavement surface characteristics, pavement safety, and ride quality.

**Keywords:** mean profile depth; gaussian mixture model; random forest model; centroid-based optimization; long-term pavement performance; machine learning model

## 1. Introduction

Pavement texture is a key factor that impacts road safety and performance, particularly skid resistance, friction, and drainage. The texture refers to the deviation of a pavement surface from a true planar surface (ISO13473-1:1997). According to (PIRAC, 1987), the road surface characteristics are classified into four basic classes - microtexture, macrotexture, megatexture, and unevenness - as a function of wavelength ($\lambda$) of the irregularities. The surface texture connects with friction, drainage, noise, brightness, wear, and comfort. Elevated textures can significantly reduce noise and improve driving safety (Yang et al., 2021; Leng et al., 2023).

Microtexture as MPD connects to road friction, influencing vehicle safety and accident rates (Tian et al., 2020). The relationship between MPD and skid resistance exhibits variability, especially at different speeds (Li et al., 2020). Higher MPD values correlate with better skid resistance, reducing the risk of accidents, especially in wet conditions. Recognizing the importance of pavement surface characteristics to ensure pavement performance, the LTPP program was initiated for some selected pavement sections throughout the US.

The LTPP program is an extensive initiative designed to provide State Highway Agencies (SHAs) with in-depth technical knowledge and resources necessary to preserve and enhance the durability of road surfaces. The program determines the impacts of diverse factors, for example, loading, environment, material properties, construction quality, and maintenance on pavement

 doi:10.20944/preprints202603.1280.v1



distress and performance, and finally establishes a national long-term pavement database to support future research and needs. (E. Elkins and Ostrom 2019).

SPS examines specific variables related to new construction, maintenance treatment, and rehabilitation activities, with approximately 1,600 pavement test sections maintained under SPS project sites (E. Elkins and Ostrom 2019). The generic SPS pavement layout, illustrated in Figure 1, consists of two transition zones next to the central lane, and the maintenance control zones are at the ends of the left and right lanes. By grouping similar pavement sections, researchers can analyze performance variations

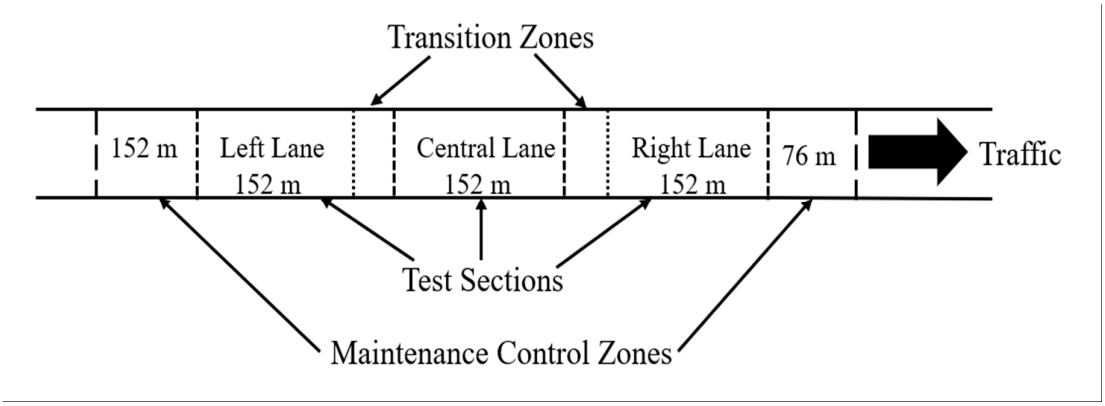


**Figure 1.** Example layout of a generic SPS Project (Source: FHWA).

For example, Sunitha et al. (2012) demonstrated that each cluster could have distinct deterioration models to predict pavement performance over time. Furthermore, Plati et al. (2019) showed that clustering MPD data to predict noise levels more reliably, is essential for urban planning and road safety. Clustering studies in pavement engineering have increasingly utilized machine learning (ML) and data-driven techniques to enhance pavement data analysis, focusing on texture, pavement condition assessment, and performance prediction. Fuzzy C-Means (FCM) algorithms have been effectively applied to categorize pavement distress parameters and reveal two distinct clusters representing good and poor pavement conditions based on a dataset from a specific road network (Gowda et al., 2023). Spatial clustering algorithms have been utilized for pavement crack segmentation and analyzing their performance under different conditions (DanWang et al., 2022).

Clustering methods like agglomerative hierarchical, partitional K-means, and fuzzy C-means algorithms identify similar traffic patterns and develop cluster average level 2 input for pavement Mechanistic-Empirical (ME) design (Li et al., 2017). Considering multiple factors like traffic and weather conditions, and their impact on pavement deterioration, probabilistic soft clustering provides better results for partitioning pavement data due to its soft clustering approach, which allows for more flexible groupings (Mukhtarli 2020). Unlike simpler models like K-means, which assume spherical clusters, GMM can make clusters of various shapes and sizes by fitting a mixture of Gaussian distributions, allowing for more accurate representation of data structures (Sampaio, R., et al., 2023, and Zhao, Y., et al., 2019). MPD profiles often contain gradual transitions with continuous variations. GMM assigns probabilities to each cluster instead of implementing hard cluster determination. In addition, due to the nature of pavement surfaces, MPD profiles exhibit a mixture of multiple distributions, making the GMM fit. The relationship between texture and factors such as traffic, weather, aggregate, and volumetric properties is intricate; hence, continued exploration in current and future studies.

The relationship between traffic volume and pavement texture is complex and involves macro and micro-texture changes. Studies have shown that texture properties are highly correlated with frictional properties of pavement, which are affected by traffic volume (Mohammad and Ismael 2021). Traffic load and volume significantly influence the texture and skid resistance, as increased traffic volumes tend to reduce the MPD of pavements in studies conducted on various asphalt pavement

 doi:10.20944/preprints202603.1280.v1



sections (Ozdemir et al., 2021). This reduction in texture depth is primarily due to the polishing effect of heavy traffic, which smoothens the pavement surface over time, thus decreasing its skid resistance (Mohammad and Ismael 2021).

Environmental factors such as temperature changes also play a key role in the texture. For instance, changes to road MPD follow a linearly increasing trend with time, influenced by Annual Average Daily Traffic (AADT) and seasonal conditions like rainfall and temperature (Edmondson et al., 2021). Extreme climatic conditions, such as high moisture and low temperatures, can cause sudden pavement failure by increasing fatigue strains in the basecourse layer, with heavy traffic loading having a minor impact (Kodippily et al., 2018).

Aggregate size, shape, and gradation collectively influence the texture and overall performance of construction materials, while proper gradation ensures optimal pavement performance. Larger aggregates tend to enhance the macrotexture of pavements, which is critical for anti-skid performance (Wu et al., 2020), and the nominal aggregate size is particularly influential in measuring surface texture levels, as it impacts the friction and noise-related properties of pavements (Praticò and Briante, 2020). The interaction between gradation and texture is complex, but gradation can be used to predict surface texture levels effectively (Praticò and Briante 2020).

The volumetric properties of asphalt resist cracking and other forms of distress, which can also lead to improved texture durability, ensuring long-lasting pavement performance. Studies have found that higher air voids can improve cracking resistance, as they allow for more flexibility and deformation under stress (Chen et al., 2023). The balance of air voids is crucial, as too few can lead to rutting, but too many can hamper the pavement's structural integrity (John et al., 2021). The same is true for binder content as well. Optimum binder content is necessary to ensure a balance between flexibility and structural integrity, contributing to the overall durability of the pavement (Slebi-Acevedo et al., 2019). Machine learning is increasingly used to identify critical variables affecting pavement performance, aiding in the prediction and maintenance of road conditions.

ML algorithms like Random Forest (RF), Artificial Neural Network (ANN), and Support Vector Machine (SVM) capture on average 15.6% more variability than traditional techniques for predicting pavement deterioration (Bashar and Torres-Machí, 2021). ANN can accurately predict pavement performance metrics like IRI, with high R-squared values and low MSE (Bashar and Torres-Machí, 2021, and Aranha et al., 2023). Similarly, RF has been effectively performed to predict the Pavement Condition Index (PCI) and IRI, demonstrating strong prediction capabilities with high R-squared values (Naseri et al., 2022, and Abdualmtalab et al., 2023). Stochastic Gradient Descent Logistic Regression (SDG-LR) has been employed to automatically detect raveling in asphalt pavement using image texture features, and this approach attained a classification accuracy of approximately 88% (Hoang, N. 2019).

The integration of clustering-based texture profiling with variable importance analysis is an area that is underexplored in the current literature. While previous studies focused on texture analysis, texture clustering with the determination of critical factors through statistical and multiple ML methods is not featured. For the large dataset, GMM might be the best clustering technique due to its flexibility and probabilistic foundation, handling clusters with distinct sizes and shapes, flexibility with overlapping clusters, likelihood-based optimization, and capability to capture hidden structures. Texture profile clustering with GMM, and integration with a considerable number of variables importance analysis, remains limited. The authors address the gap in the research to develop methods that not only cluster analysis of texture but also assess the importance of different factors that influence the texture.

## 2. Research Objectives

This study aims to cluster the MPD and explore the important factors to make a generalized contribution about different levels of MPD. The author completed the aim by grouping the MPD profiles into four clusters and developing statistical and multiple robust categorical ML algorithms for evaluating key factors from traffic, aggregate, volumetric properties, and weather parameters that

 doi:10.20944/preprints202603.1280.v1



affect pavement texture variability at distinct levels. An ordered logistic regression for statistical model and multiple algorithms using K-nearest neighbor, random forest, extra trees, extreme gradient boosting, cat boosting, neural network, and weighted ensemble algorithm for ML models. The findings from this study will provide transportation agencies with a data-driven approach to better understand pavement surface characteristics, pavement safety, and ride quality. Additionally, the study will contribute to prioritizing maintenance decisions and predicting pavement deterioration by identifying critical factors in similar pavement sections with similar wear patterns.

## 3. Methodology

The study adopted a multi-stage methodology for pavement surface texture (MPD) and identified key influencing factors. The process involves raw data processing, filtering, MPD profile calculation, texture clustering, representative profile making, and lastly applying statistical and multiple machine learning models. Figure 2 displays the whole process step by step.

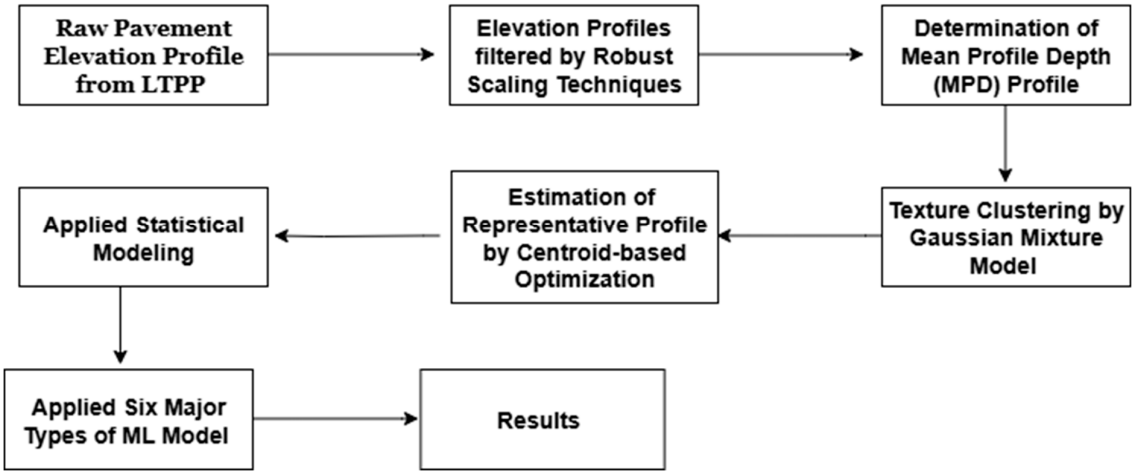


**Figure 2.** Methodological Framework for MPD Clustering and Influencing Factor Identification.

## 4. Data Collection and Processing

*4.1 Data Collection*

The research considered the seven US states named Alabama, Arizona, Delaware, Florida, New York, Ohio, and Utah, each for two SPS test sections and one SPS section for Montana and Pennsylvania. Each SPS pavement section was gathered in the left, right, and central lanes to ensure the completeness of the same pavement section according to the layout of the generic SPS project in Figure 1. Of the 9 US states, sixteen full SPS sections are collected, considering forty-eight sections in each year of 1998, 2001, 2004, and 2005, for a total of 192 pavement sections. These pavement sections were gathered as .erd files and analyzed by ProVAL 3.61 to get elevation data for 152 meters of each section length. The elevation data were divided into 0.025m intervals to get 6081 data points on each pavement profile. Later, the MPD profiles were evaluated from the elevation profiles.

The research accumulated eighteen pavement-associated factors, which were classified into four categories as traffic, weather, aggregate, and asphalt volumetric properties. The traffic categories consisted of one pavement evaluation matrix named International Roughness Index (IRI), Annual Average Daily Truck Traffic (AADTT), and 18-kip ESAL. Similarly, three major factors, including precipitation, temperature, and freezing index, were the representatives of the weather category. Most eight factors were lead on aggregate data collection, including untreated subgrade (Untr. Subgrade), #4 sieve, #200 sieve, geological classification of soil (Soil Geo Class), Bulk Specific Gravity (GSB) for both Coarse Aggregate (CA) and Fine Aggregate (FA), and the absorption of CA and FA. To emphasize the volumetric properties of Asphalt, four critical asphalt variables were collected:

 doi:10.20944/preprints202603.1280.v1



Maximum Specific Gravity (GMM) and Bulk Specific Gravity (GSB) of asphalt, the other two volumetric properties were asphalt content mean, and percent air voids. Notably to mention, all the pavement-associated variables were annual averages on their respective units. The data collection of these eighteen factors was maintained on each pavement section with respective pavement section IDs, and in the corresponding state, year, and lane sections.

*4.2. Data Preprocessing*

Pavement surface elevation data display significant variations due to measurement inconsistencies, localized surface roughness, and environmental factors. These datasets frequently contain outliers from extreme wear, irregular pavement surface conditions, and sensor noise. The traditional normalization or standardization method may not be the best fit; rather, robust scaling techniques are widely used in data preprocessing due to their ability to effectively handle outliers and non-Gaussian distributions. The robust scaling uses the median and interquartile range (IQR), addressed in Equation 1, to ensure that the outliers proportionately influence the transformed data. This makes it particularly advantageous in datasets with high variability by improving numerical stability for machine learning models, preserving the relative importance of feature differences, mitigating the effects of outliers, maintaining the natural structure of data distribution, and enhancing the accuracy and reliability of clustering, regression, and classification.

The robust scaling transformation refers to:

$$X_{scaled} = \frac{X - X_{median}}{X_{IQR}} \quad (1)$$

Addressed as,

- $X_{median}$, the Median of the dataset that is resistant to outliers
- $X_{IQR}$, Interquartile range (Q3 – Q1) captures variability without interpreting extreme values
- $X_{scaled}$, resulting data, scaled proportionally to the interquartile range

*4.3. Determination of Mean Profile Depth*

To assess pavement texture characteristics, the research computed the Mean Profile Depth (MPD) from pavement elevation profile data using Python. The SPS pavement section length is 152m, with a data interval is 0.025m. Hence, the MPD profile was determined at a 0.5m interval with the same section length by making two baselines of 0.025m intervals. After that, each baseline was determined by the peak level and average level to calculate MPD referencing in Figure 3.

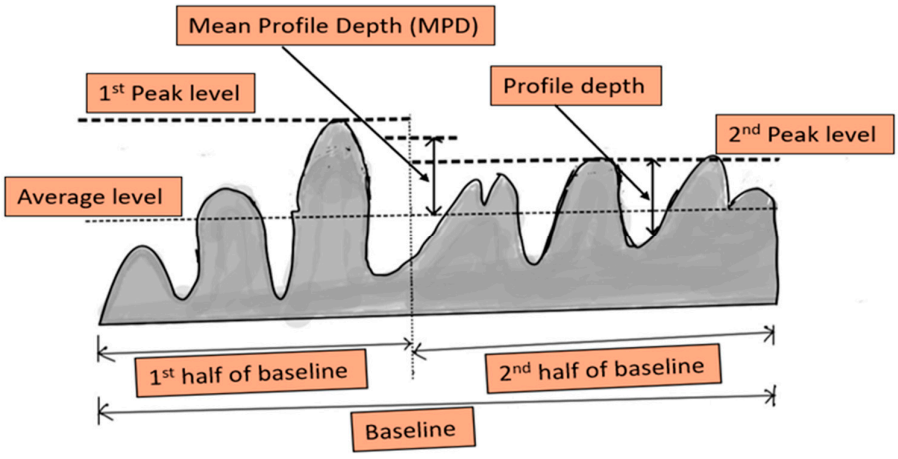


**Figure 3.** Display the concept of baseline, profile depth, and MPD (ISO 13473-1).

 doi:10.20944/preprints202603.1280.v1



The MPD computation follows according to ASTM E1845 for each profile to determine the arithmetically averaged two peak levels minus the average profile level, which was addressed in Equation 2. By implementing this methodology in Python, the research team efficiently processes the large dataset of pavement elevation profiles, ensuring accurate and automated MPD estimation. This MPD computation forms the basis for subsequent clustering analyses using GMM to identify distinct pavement texture groups.

$$MPD = \frac{Peak\ level\ (1st) + Peak\ level\ (2nd)}{2} - Average\ level \quad (2)$$

## 5. Texture Clustering

The research approached the GMM for clustering MPD profiles because of the continuous nature of pavement surface variations. Rigid clustering approaches assume well-separated groups, but MPD profiles often exhibit gradual transitions between smooth and rough textures, making strict clustering assignments less suitable. While K-means assumes clusters are equally shaped and spaced, GMM considers each cluster as a multivariate Gaussian distribution, allowing it to capture elliptical and irregular patterns present in real-world MPD values. GMM's probabilities framework captures soft clustering, which computes each pavement section as a probability of belonging to multiple clusters. Thus, flexible classification and covariance matrices make subtle distinctions between pavement surface conditions while preserving the natural complexity of surface texture data. The probability density function (PDF) of a GMM with K components is expressed in Equation 3.

$$p(x) = \sum_{k=1}^{K} \pi_k . \mathcal{N}(x|\mu_K, \sum_k) \quad (3)$$

Where:

- $\pi_k$, the mixing coefficient for cluster k satisfying $\sum_{k=1}^{K} \pi_k = 1$
- $\mathcal{N}(x|\mu_K, \sum_k)$, the multivariate Gaussian distribution with mean $\mu_K$ and covariance $\sum_k$
- $x$, the feature vector as MPD values.

The GMM is trained using the Expectation-Maximization (EM) algorithm, an iterative approach to estimating the parameters of the Gaussian distributions by maximizing the likelihood function as addressed in equation 4. In the Expectation step (E-step), the algorithm calculates the probability that each Gaussian component K has for each data point $x_i$. The probability represents the likelihood of each generated point of the current model parameters. In the maximization step (M-step), the probability calculation in the E-step regulates the parameters of each Gaussian component, including the mean, mixing coefficient, and covariance. The regulated parameters update the weighted average of data points. The iterative E-M approach refines the model parameters, with each step improving the model fitness till the likelihood becomes negligible. The log-likelihood of the observed data given the model parameters is:

$$\log L(\theta) = \sum_{i=1}^{N} \log \left( \sum_{k=1}^{K} \pi_k \mathcal{N}(x_i|\mu_k, \sum_k) \right) \quad (4)$$

Where,

- $\theta = (\pi_k, \mu_k, \sum_k)$, the model parameters,
- $\mathcal{N}$, the number of data points

### *5.1. Clustering Results*

In this study, the author determined the optimal number of clusters for the GMM using the Silhouette Score, rather than relying on the traditional Bayesian Information Criterion (BIC) or Akaike Information Criterion (AIC). The uniqueness of the research determined the clustering by

 doi:10.20944/preprints202603.1280.v1



maintaining the quality of clustering in terms of separation and compactness, and the Silhouette score directly measures clustering quality by considering both intra-cluster cohesion and inter-cluster separation. The Silhouette score computed on Equation 5 for any given data point $i$:

$$S(i) = \frac{b(i) - a(i)}{\max(a(i), b(i))} \quad (5)$$

Where:

- $a(i)$, the average intra-cluster distance
- $b(i)$, the lowest average intra-cluster distance

Figure 4 represents the optimal number of clusters. At clusters 2 and 3, the score was 0.325 and 0.355, and in cluster 4, the Silhouette score rose to 0.725, indicating most scores, well-defined and interpretable clusters. At cluster 5, the score is slightly lower than cluster 4, and clusters 6 to 10 varied the score by 0.3 to 0.35. High Silhouette score with lower clusters might indicate underfitting, thus, four clusters of MPD with a silhouette score of 0.725 also overcome the underfitting issues, meaning the MPD profiles are well-separated and compact.

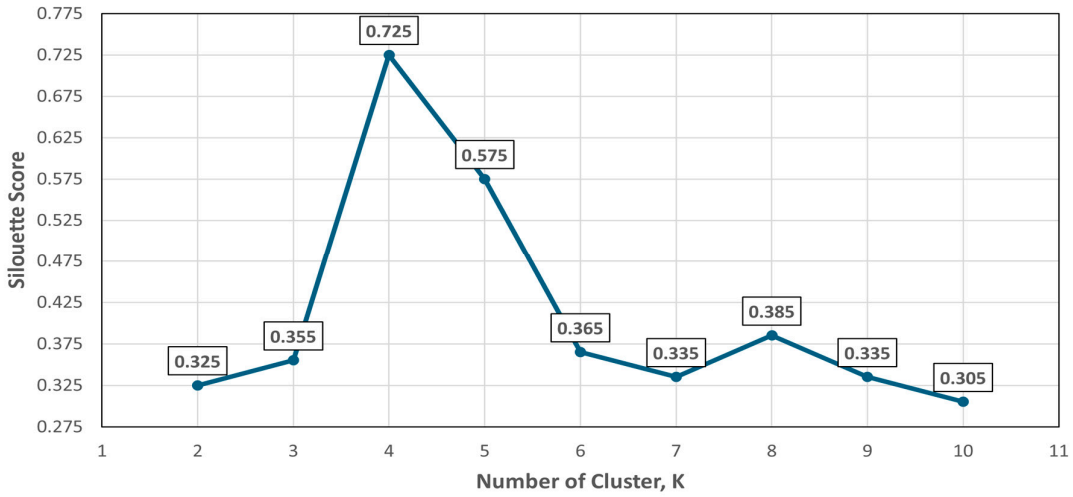


**Figure 4.** Determination of Optimal Cluster Number.

## 6. Estimation of Cluster-Representative Profiles

From GMM, the research got four (K = 4) clusters, where each cluster had varied MPD profiles. In Cluster-0: 49 profiles, Cluster-1: 116, Cluster-2: 12, Cluster-3: 15, averaging 48 profiles per cluster, with the largest number of MPD profiles in Cluster-1. This variation reflected the diversity in pavement textures and reinforced the necessity of a structured medoid-based computation approach. The medoid-based representative profile ensured the selected profile was an actual and existing MPD measurement rather than the traditional mean approach to preserving real-world interpretability.

An exhaustive search optimization technique among the current cluster members to compute the cluster centroid, named the K-medoid-type algorithm. This approach enables flexible modeling of clusters, even those with significantly varying variances (Olszewski and Šter, 2014). A four-step approach in Figure 5, started with the objective function to apply K-medoids, formulating the optimization problem, solving the optimization problem, and the decisive step was implementing the solution in Python.

 doi:10.20944/preprints202603.1280.v1



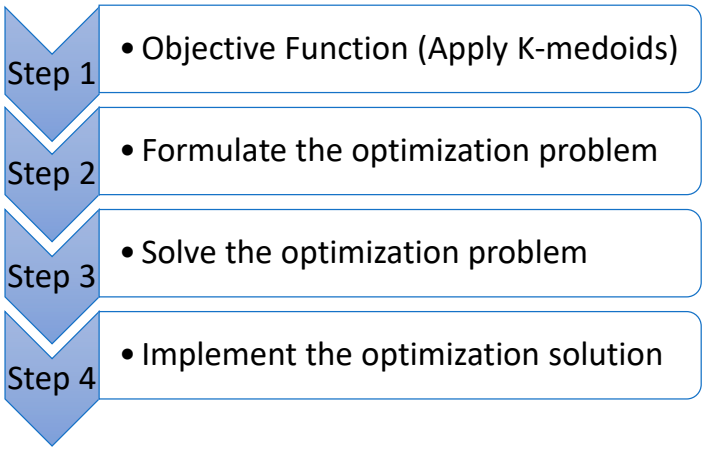


**Figure 5.** Steps of Centroid-based Optimization.

The objective function is a mathematical formulation intended to minimize or maximize certain criteria to determine the most representative section within a cluster. Applying the K-medoid algorithm to the chosen section is expected to minimize the section distance to all other sections within the cluster. Hence, serving as the pivotal point based on its proximity to the other sections, expressed in equation 6 as the objective function.

$$\text{Minimize } f(Xj) = \sum_{k=1}^{m} Distance\ (X_j, X_k) \quad (6)$$

Referred to,

- $X_j$, feature vector of section j
- $X_k$, all other sections within the cluster

The research expressed the optimization problem as in equation 7

$$X_j \epsilon\ Cluster_j^{min}\ f(X_j) \quad (7)$$

Where,

- $f(X_j)$, the objective function developed by the most significant criteria

Authors introduced the gradient descent algorithm as an advanced optimization technique for large datasets. The algorithm iteratively adjusts parameters to minimize the error function to achieve a more computationally efficient solution. This transition facilitated faster convergence and improved the efficiency and precision of the model by extracting meaningful insights from the data. Finally, the writers initiated the deployment by computing the Euclidean distance between pairs of points. For each cluster, we calculated the centroid by averaging the feature values of its sections. Later, we used Python to calculate the distance from each section to the centroid and selected the closest one. Repeating this for all clusters, we assembled a new data frame containing four representative pavement profiles in Figure 4.

*6.1. Cluster-Representative Profiles Results*

According to Meegoda J.N et al. (2002), low macrotexture refers to MPD values lower than 1.5mm, and high macrotexture refers to MPD values higher than about 1.5mm. Cluster_0, labeled Fine Texture with an MPD range of 0.55-0.7mm, represented pavements with minimal texture, indicating smoother surfaces and reduced friction in Figure 6.

 doi:10.20944/preprints202603.1280.v1



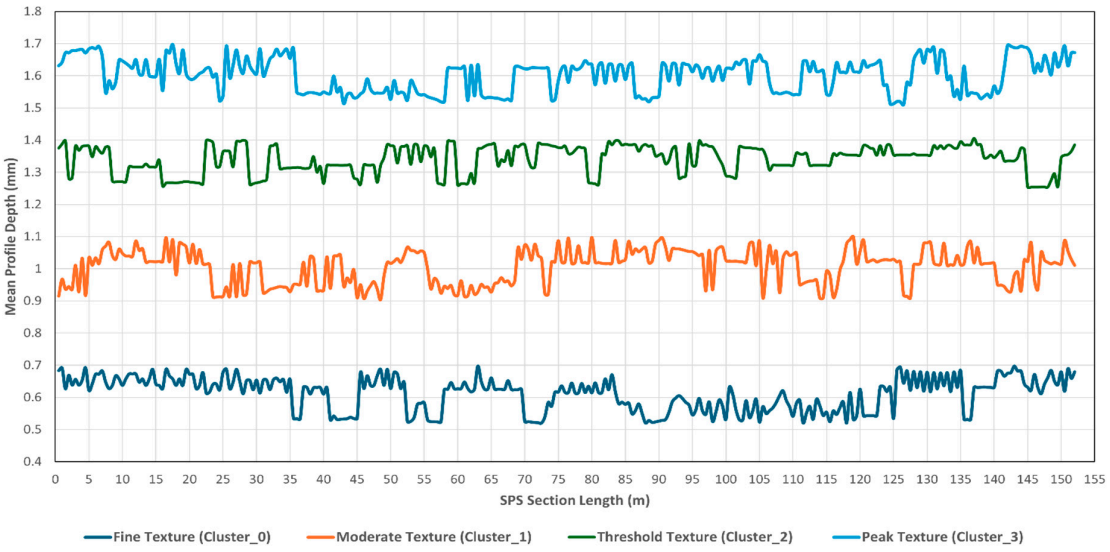


**Figure 6.** Cluster-Representative Profiles.

Cluster_1 (0.9-1.1mm) represents a moderate-low texture profile, indicating slightly rougher surfaces that balance friction and rolling resistance. Cluster_2, spanning 1.25-1.4mm, classified as threshold texture, shows enhanced skid resistance with limited drainage efficiency. Finally, cluster_3, ranging from 1.55-1.7mm, indicates a high texture, where increased macrotexture improves both friction and water drainage, essential for wet-weather safety. This clear cluster separation offers valuable insights into data-driven pavement maintenance and safety evaluations

## 7. Statistical Model

*7.1 Independent Variables*

The research considered eighteen factors, including traffic, weather, aggregate, and volumetric properties, addressed in Table 1. Initially, we performed a rigorous statistical analysis named ordered logistic regression to quantify their individual and combined effects. Later, we proceeded with fourteen different ML models to capture complex and non-linear relationships of data and identify hidden patterns among dependent and independent variables.

**Table 1.** Independent Variables.

| Factors Type | Factors | Description |
|---|---|---|
| Pavement | IRI | International Roughness Index section average (m/km) |
| Traffic | AADTT | Annual average daily truck traffic (No.) |
| | 18-Kip ESAL | Standard truck loading (KESAL) |
| Weather | Precipitation | Annual average precipitation (mm) |
| | Temperature | Annual average temperature (deg C) |
| | Freezing index | Annual average freeze index (deg C deg days) |
| Aggregate Properties | Untr. Subgrade | Untreated subgrades considering ten categories |
| | #4 sieve | Percentage of aggregate passing through #4 sieve |
| | #200 sieve | Percentage of aggregate passing through #200 sieve |
| | Soil geo class | Soil geological classification regarding four categories |

 doi:10.20944/preprints202603.1280.v1



| | | |
|---|---|---|
| | GSB of CA | Bulk specific gravity of coarse aggregate |
| | Absorption of CA | Absorption of coarse aggregate |
| | GSB of FA | Bulk specific gravity of fine aggregate |
| | Absorption of FA | Absorption of fine aggregate |
| Volumetric Properties | GMM of Asphalt | Maximum Specific Gravity of Asphalt |
| | GSB of Asphalt | Mean Bulk Specific Gravity of Asphalt |
| | Asphalt Content | Asphalt Content Mean |
| | Percent Air Void | Percent Air Void Mean |

*7.2. Ordered Logistic Regression*

An ordered logistic regression model is a variant of logistic regression designed for ranked ordinal data with an assumption of proportional odds. Equation 8 (Williams, 2016) presented the general form of the generalized ordered logit model, which relates a response variable Y with M ordinal categories to a set of predictors X. Since the response variable Cluster exhibited ordinal nature with increasing levels from 0 to 3, the ordered model was developed to investigate critical factors using the proportional odds logistic regression (polr) function in R.

$$P(Y_i < j) = \frac{\exp(\alpha_j + X_i\beta_j)}{1+[\exp(\alpha_j + X_i\beta_j)]}, j = 1,2,\dots,M-1 \quad (8)$$

where,

- $X_i\beta_j$, the sum of the product of the value and coefficients of all predictors
- $\alpha_j$, threshold value of each ordinal category j.

Multicollinearity among predictors can significantly worsen model accuracy in statistical regression analysis. Variance Inflation Factor (VIF) is commonly used to detect multicollinearity, with values higher than 5 to 10 indicating multicollinearity issues (Kim, 2019). An initial analysis of 18 predictor variables revealed significant multicollinearity, observed from high VIF (> 10). Ten variables were selected based on their lower intercorrelations, practical relevance to pavement texture, and compatibility with ordered logit modeling. The selected variables were IRI, AADTT, 18-Kip ESAL, Precipitation, Temperature, Soil Subgrades, #4_Sieve, GSB of CA, GMM of Asphalt, and Asphalt Content – a well-rounded combination of pavement, traffic, weather, aggregate, and volumetric properties.

*7.3. Model Evaluation and Fit Statistics*

The overall evaluation metrics showed moderate results, but adding predictors improved the statistical model compared to the intercept-only (null) model, as shown in Table 2.

**Table 2.** Evaluation Metrics Result and Description.

| Metric | Value | Description |
|---|---|---|
| Accuracy | 58.46% | the model correctly classifies 58.46 % of the clusters |
| Weighted Precision | 52.25% | the model accurately predicted 52.25 % of the clusters |
| Weighted Recall | 58.46% | the model correctly made a true cluster of 58.46 % |

 doi:10.20944/preprints202603.1280.v1



| | | |
|---|---|---|
| Weighted F1-score | 54.90% | the harmonic mean of weighted precision and recall, indicating a moderate balance between identifying true clusters and avoiding false positives. |
| McFadden's pseudo-$R^2$ | 21% | a 21 % increase in explanatory power compared to the null model. |
| Cox & Snell $R^2$ | 35% | the model explains 35-40 % of the variance in pavement texture classification, indicating improvement in the model's explainability compared to the null model. |
| Nagelkerke $R^2$ | 40% | |
| Log-Likelihood | -52.71 | improvement over the null model's fit, but with a marginal statistical significance compared to the traditional threshold of 0.05. |
| Likelihood Ratio Test | $\chi^2$ = 27.97, p = 0.062 | |

*7.4. Model Results*

Table 3 represents the coefficients, standard errors, t-values, and p-values for all the predictor variables listed in the model.

**Table 3.** Ordered Logistic Regression Results for Pavement Texture Clusters.

| **Parameter** | **Coefficient** | **Std. Error** | **t-value** | **p-value** | **Significance** |
|---|---|---|---|---|---|
| IRI | 6.686 | 0.823 | 8.119 | $4.68\times10^{-16}$ | *** |
| AADTT | $5.078\times10^{-3}$ | $8.49\times10^{-4}$ | 5.980 | $2.24\times10^{-9}$ | *** |
| 18-Kip ESAL | $-8.313\times10^{-4}$ | $1.26\times10^{-3}$ | -0.659 | $5.10\times10^{-1}$ | |
| Precipitation | $2.491\times10^{-3}$ | $1.10\times10^{-3}$ | 2.261 | $2.38\times10^{-2}$ | * |
| Temperature | 0.552 | 0.064 | 8.662 | $4.63\times10^{-18}$ | *** |
| Untr_Subgrade (Clayey Sand with Gravel) | -17.772 | 0.711 | -24.999 | $6.25\times10^{-138}$ | *** |
| Untr_Subgrade (Sand) | 7.572 | 0.741 | 10.219 | $1.63\times10^{-24}$ | *** |
| Untr_Subgrade (Sand with Silt and Gravel) | -27.877 | 0.842 | -33.108 | $2.27\times10^{-240}$ | *** |
| Untr_Subgrade (Sandy Lean Clay) | -10.336 | 1.040 | -9.943 | $2.72\times10^{-23}$ | *** |
| Untr_Subgrade (Sandy Silt) | -8.837 | 0.712 | -12.406 | $2.42\times10^{-35}$ | *** |
| Untr_Subgrade (Silt) | -5.578 | 0.240 | -23.194 | $5.21\times10^{-119}$ | *** |
| Untr_Subgrade (Silty Clay) | -8.011 | 0.972 | -8.240 | $1.72\times10^{-16}$ | *** |
| Untr_Subgrade (Silty Sand) | 5.250 | 0.776 | 6.768 | $1.30\times10^{-11}$ | *** |

 doi:10.20944/preprints202603.1280.v1



| | | | | | |
|---|---|---|---|---|---|
| Untr_Subgrade (Silty Sand with Gravel) | -28.156 | 0.777 | -36.260 | $6.99\times10^{-288}$ | *** |
| #4_Sieve | 0.079 | 0.051 | 1.549 | $1.21\times10^{-1}$ | |
| GSB of CA | -51.662 | 0.427 | -121.053 | $<1.00\times10^{-320}$ | *** |
| GMM of Asphalt | -150.092 | 0.415 | -361.505 | $<1.00\times10^{-320}$ | *** |
| Asphalt Content | -17.826 | 0.754 | -23.642 | $1.42\times10^{-123}$ | *** |

Note: *p<0.05; **p<0.01; and ***p<0.001.

The statistical results revealed several significant factors influencing pavement texture clustering. A higher positive coefficient indicates a strong positive association with higher texture clusters, and vice versa. IRI had a coefficient of 6.686, indicating that rougher pavements are more likely to be categorized as higher texture clusters. Similarly, traffic parameters like AADTT (coefficient = $5.078\times10^{-3}$), and environmental factors like precipitation (coefficient= $2.491\times10^{-3}$) and temperature (coefficient = 0.552) demonstrated that higher traffic frequency, precipitation, and temperature might lead to worse mean profile depth texture conditions.

Meanwhile, different subgrade soil types showed different effects on pavement texture. For example, “Sand" (coefficient = 7.572) and "Silty Sand" (coefficient = 5.250) were associated with higher texture clusters, while "Sand with Silt and Gravel" (coefficient = -27.877) and "Silty Sand with Gravel" (coefficient = -28.156) were associated with lower texture clusters. The influencing parameters were the material parameters such as GSB of CA (coefficient = -51.662), GMM of Asphalt (coefficient = -150.092), and Asphalt Content (coefficient = -17.826), which confirmed that higher quality materials significantly contribute to better pavement texture.

*7.5. Predictive Model for Cluster Classifications*

Based on the coefficients of regression results, a predictive model for pavement texture clusters is formulated by computing the linear predictor (η) as:

$$\eta = 6.686 \times \text{IRI} + 0.00508 \times \text{AADTT} - 0.000831 \times \text{18-Kip ESAL} + 0.00249 \times \text{Precipitation} + 0.552 \times \text{Temperature} + \beta_{\text{soil}}(\text{Soil Type}) + 0.0788 \times \text{\#4\_Sieve} - 51.66 \times \text{GSB of CA} - 150.09 \times \text{GMM of Asphalt} - 17.83 \times \text{Asphalt Content} \quad (9)$$

where $\beta_{\text{soil}}$ represents the coefficient for the specific subgrade soil type.

The probability of each pavement texture cluster can be determined using the cumulative probability in Equation 9 (Lee, 1992),

$$P(Y \leq j) = \frac{1}{1+\exp\ -(\alpha_j+\eta)} \quad (10)$$

where,

- j = 1, 2, ……., M-1

The model results provided three threshold values ($\alpha_j$) of -589.744, -584.993, and -584.180 for clusters 0|1, 1|2, and 2|3, respectively. The probability of each cluster can be determined from the difference of two cumulative probabilities, as shown in the following equations. For a given set of predictor values, the cluster with the highest probability is the predicted cluster.

 doi:10.20944/preprints202603.1280.v1



$$P(\text{Cluster} = 0) = \frac{1}{1+\exp(\eta+589.74)} \quad (11)$$

$$P(\text{Cluster} = 1) = \frac{1}{1+\exp(\eta+584.99)} - \frac{1}{1+\exp(\eta+589.74)} \quad (12)$$

$$P(\text{Cluster} = 2) = \frac{1}{1+\exp(\eta+584.18)} - \frac{1}{1+\exp(\eta+584.99)} \quad (13)$$

$$P(\text{Cluster} = 3) = 1 - \frac{1}{1+\exp(\eta+584.18)} \quad (14)$$

## 8. Machine Learning Model

While the ordered logit model identified critical factors, but limitations in handling collinear predictors and capturing nonlinear relationships. To address these limitations, we developed fourteen different ML models, which are robust to predictor collinearity and effective in capturing non-linear relationships critical for accurate cluster prediction.

The statistical analysis selected ten factors out of eighteen for multicollinearity (VIF >10). Thus, the research team was more curious to explore these ten variables through multiple machine learning models. Non-linear relationships between variables, modeling intricate variable interactions, handling high-dimensional datasets effectively, identifying hidden patterns, and enhancing predictive accuracy were critical to understanding the relationship between these ten factors and texture. We studied fourteen different ML models within six major types of ML algorithms, listed in parentheses. We also employed ensemble learning algorithms to combine predictions in the final stacking layer.

- K-nearest neighbor algorithm (e.g., "KNeighborsDist" and "KNeighborsUnif")
- Radom forest algorithm (e.g., "RandomForestEntr" and "RandomForestGini")
- Extreme random tree algorithm (e.g., "ExtraTreesEntr" and "ExtraTreesGini")
- Boosting tree algorithm (e.g., "XGBoost," "CatBoost," "LightGBM," "LightGBMXT," and "LightGBMLarge")
- Neural network algorithms (e.g., "NeuralNetFastAI" and "NeuralNetTorch")
- Ensemble learning algorithms (e.g., "WeightedEnsemble_L2")

### *8.1. K-Nearest Neighbors (K-NN) Algorithm*

The K-Nearest Neighbors (K-NN) algorithm assigns an unlabeled observation to a class based on the majority vote of its K nearest labeled neighbors, using proximity as the primary criterion for classification (Géron, 2019). The K-NN classifier supports multiple predictors, enabling flexible classification. Its performance depends on the chosen distance metric and weighting scheme, which influence accuracy. Weighted KNN with uniform weights and distance-weighted KNN models are trained based on different weight setting methods, K nearest neighbor instances. KNN algorithms with uniform weights and distance-related weights are denoted as "KNeighborsUnif" and "KNeighborsDist", respectively.

### *8.2. Random Forest (RF) Algorithm*

The Random Forest algorithm (Chatterjee et al. 2024, Munna et al. 2025, Rana et al. 2025, Desai and Chatterjee. 2026) uses Bagging (Bootstrap Aggregating) to create multiple subsets of the data and uses Decision Trees to train these subsets. A majority vote across all trained trees determines the final prediction, enhancing model stability and reducing overfitting. The main advantages of Random Forest over other machine learning algorithms include high accuracy on large datasets, resilience to class imbalance, and powerful performance in handling missing values and noisy data (Breiman, 2001). Shannon entropy and Gini index commonly measure node purity for categorical variables –

 doi:10.20944/preprints202603.1280.v1



lower values indicate higher homogeneity. In classification, random forest using these criteria was denoted as "RandomForestEntr" and "RandomForestGini," respectively.

*8.3. Extreme Random Tree Algorithms*

The Extra-Trees algorithm, introduced by Geurts et. Al. (2006) uses strong randomization in attribute and cut-point selection, building trees less dependent on the training data. It reduces variances more effectively than traditional decision trees while remaining computationally efficient. Unlike Random Forests, Extra-Trees train each tree on the full dataset and randomly select cut-points, resulting in highly diverse yet computationally fast models. It used Entropy and Gini impurity as splitting criteria for classification, labeled as "ExtraTreesEntr" and "ExtraTreesGini."

*8.4. Boosting Tree Algorithms*

Gradient Boosted Decision Trees (GBDT) (Chatterjee et al. 2024, Munna et al. 2025, Rana et al. 2025, Desai and Chatterjee. 2026) is a powerful ensemble method for classification and regression that builds trees sequentially, with each tree correcting the residuals of the previous, enhancing prediction accuracy (Si et al. 2017). Recent advancements, such as LightGBM, have introduced optimization techniques like Gradient-based One-Side Sampling (GOSS) and Exclusive Feature Bundling (EFB) to enhance computational efficiency and scalability, particularly for large datasets (Machado et al. 2019). Along with LightGBM, the authors studied LightGBMXT, LightGBMLarge, XGBoost, and CatBoost.

*8.5. Neural Network Algorithms*

Neural networks, mimicking the human brain, are core to modern machine learning and AI, using interconnected layers to model complex and non-linear data patterns (Liu and Jiang, 2021, Chatterjee et al. 2026a, Chatterjee et al. 2026b). Deep Learning (DL) has seen breakthroughs in neural networks by introducing architectures like Convolutional Neural Networks (CNNs) for image processing and Recurrent Neural Networks (RNNs) for sequential data like speech and text (Alzubaidi et al. 2021). Innovations such as the transformer in Natural Language Processing (NLP) and Generative Adversarial Networks (GANs) for image processing highlight the application of neural networks across domains. Despite their success, ongoing research aims to improve their efficiency, scalability, and interpretability, ensuring their broader adoption across industries (Liu and Jiang, 2021). The neural network algorithm executed with PyTorch and FastAI was denoted as "NeuralNetTorch" and "NeuralNetFastAI."

*8.6. AutoGluon Multi-layer Weighted Ensembling Model*

The AutoGluon Multilayer Weighted Ensembling Model is an advanced AutoML framework that enhances predictive performance by combining multiple machine learning models using a multi-layer stacking strategy (Qi et al. 2021). Unlike traditional assembling methods, AutoGluon integrates various base models, including Random Forest, Gradient Boosting Decision Trees, Neural Networks, and k-Nearest Neighbors, and refines them through a layered ensembling process, where higher-layer models learn from lower-layer model outputs (Erickson et al. 2020). It improves robustness and accuracy by automating model selection, hyperparameter tuning, and data preprocessing, minimizing manual intervention while ensuring efficient training and performance enhancement (Qi et al. 2021). Its multi-layer ensembling strategy consistently outperforms traditional AutoML frameworks and efficient management of large-scale datasets with complex feature interactions (Qi et al. 2021).

*8.7. Results*

The study developed multiple ML models include K-nearest neighbor algorithm (e.g., "KNeighborsDist" and "KNeighborsUnif"), random forest algorithms (e.g., "RandomForestEntr" and "RandomForestGini"), extreme random tree algorithms (e.g., "ExtraTreesEntr" and

 doi:10.20944/preprints202603.1280.v1



"ExtraTreesGini"), boosting tree algorithms (e.g., "XGBoost", "CatBoost", "LightGBM", "LightGBMXT", and "LightGBMLarge"), neural network algorithms (e.g., "NeuralNetFastAI" and "NeuralNetTorch"), and the AutoGluon (Ver. 0.7.0) weighted ensembling model (e.g., "WeightedEnsemble_L2"). The mean profile depth clustering and pavement-associated factors were randomly selected, of which 80% were used for training and 20% for testing.

The leaderboard in Table 4 demonstrated a view of the trained ML models along with their performance. We arranged the performance ranking by each classification model based on the testing scores (Score_Test) and validation scores (Score_Val) measured by predictive probability in terms of the log-loss of each model. Fit_Order is the predefined order of the set of models based on their performance. Notably, the two best algorithms, WeightedEnsemble_L2 and KNeighborsDist, with highest classification results, where the score_test values were all over 0.846154. In addition, the tree-based algorithms - RandomForestEntr, RandomForestGini, ExtraTreesEntr, ExtraTreesGini – showed promising classification results as the Score_test values were 0.794872. In boosting tree algorithm overall performance was good except for CatBoost. But, the non-tree-based models, NeuralNetFastAI and NeuralNetTorch displayed worse predictive performance with larger log-loss.

**Table 4.** Machine Learning Models Results.

| Model | Score_Test | Score_Val | Fit_Order |
|---|---|---|---|
| WeightedEnsemble_L2 | 0.846154 | 0.903226 | 14 |
| KNeighborsDist | 0.846154 | 0.903226 | 2 |
| RandomForestEntr | 0.794872 | 0.870968 | 10 |
| RandomForestGini | 0.794872 | 0.870968 | 9 |
| ExtraTreesEntr | 0.794872 | 0.870968 | 7 |
| ExtraTreesGini | 0.794872 | 0.870968 | 9 |
| XGBoost | 0.769231 | 0.903226 | 11 |
| LightGBM | 0.769231 | 0.903226 | 5 |
| LightGBMXT | 0.769231 | 0.903226 | 4 |
| LightGBMLarge | 0.769231 | 0.903226 | 13 |
| CatBoost | 0.692308 | 0.838710 | 8 |
| KNeighborsUnif | 0.641026 | 0.741935 | 1 |
| NeuralNetFastAI | 0.615385 | 0.774194 | 3 |
| NeuralNetTorch | 0.538462 | 0.612903 | 12 |

*8.8. Feature Importance*

Determining feature importance in machine learning or deep learning is crucial to enhancing model interpretability, optimizing performance, and extracting domain-specific insights. By identifying which features most significantly influence model predictions, researchers and practitioners can better understand the underlying patterns captured by the algorithm. Hence, the model output could be aligned with domain expertise and eliminate the irrelevant variables to make more efficient and generalized models.

 doi:10.20944/preprints202603.1280.v1



**Table 5.** Feature Importance of Machine Learning Models.

| Variables | IRI | AADTT | 18_Kip_ESAL | Precipitation | Temperature | Untr_ | #4_Sieve | GSB_of_CA | GMM_of_ | Asphalt_ Content |
|---|---|---|---|---|---|---|---|---|---|---|
| KNeighborsDist | 0.006 | 0.343 | 0.233 | 0.359 | 0.014 | 0 | 0.021 | 0.007 | 0.007 | 0.006 |
| KNeighborsUnif | 0 | 0.359 | 0.227 | 0.413 | 0 | 0 | 0 | 0 | 0 | 0 |
| RandomForestEntr | 0.067 | 0.173 | 0.04 | 0.667 | 0 | 0 | 0.013 | 0 | 0.027 | 0.013 |
| RandomForestGini | 0.052 | 0.078 | 0 | 0.818 | 0 | 0 | 0.039 | 0 | 0.013 | 0 |
| ExtraTreesEntr | 0 | 0.314 | 0.271 | 0.243 | 0.1 | 0 | 0.028 | 0.014 | 0.028 | 0 |
| ExtraTreesGini | 0.047 | 0.25 | 0.328 | 0.156 | 0.141 | 0 | 0.031 | 0.031 | 0.016 | 0 |
| XGBoost | 0.325 | 0.137 | 0.071 | 0.368 | 0.053 | 0.023 | 0.023 | 0 | 0 | 0 |
| CatBoost | 0.286 | 0.082 | 0.095 | 0.359 | 0.069 | 0.033 | 0 | 0.029 | 0.016 | 0.029 |
| LightGBM | 0.297 | 0.155 | 0.015 | 0.335 | 0.055 | 0 | 0.042 | 0.028 | 0.063 | 0.008 |
| LightGBMXT | 0.255 | 0.115 | 0.045 | 0.033 | 0.069 | 0 | 0.047 | 0.033 | 0.063 | 0.041 |
| LightGBMLarge | 0.238 | 0.153 | 0.086 | 0.253 | 0.104 | 0 | 0.013 | 0.063 | 0.084 | 0.006 |
| NeuralNetFastAI | 0.227 | 0.078 | 0.038 | 0.116 | 0.107 | 0 | 0.105 | 0.065 | 0.111 | 0.156 |
| NeuralNetTorch | 0.198 | 0.213 | 0.591 | 0 | 0 | 0 | 0 | 0 | 0 | 0 |
| WeightedEnsemble_L2 | 0.006 | 0.343 | 0.233 | 0.359 | 0.014 | 0 | 0.022 | 0.007 | 0.008 | 0.006 |
| Total Relative | 2.004 | 2.793 | 2.273 | 4.479 | 0.726 | 0.056 | 0.384 | 0.277 | 0.436 | 0.265 |

According to Table 5, precipitation was the most critical variable that appeared among the top four variables for all fourteen ML algorithms, and the other three major factors were AADT, 18-Kip ESAL, and IRI. The results were similar in a real-world perspective, as those factors were affected in

 doi:10.20944/preprints202603.1280.v1



pavement texture, as we discussed in the literature review section in "Pavement Texture and Associated Factors." Environmental factors such as rainfall affect the texture and skid resistance of pavement (Edmondson et al., 2021). Traffic load and volume significantly influence the mean profile depth as increased traffic volume tends to reduce the MPD value (Ozdemir et al., 2021), and pavement experiences more traffic, both the roughness and the texture depth tend to be reduced.

## 9. Conclusions

In this study, researchers collected 192 pavement profiles and eighteen pavement factors throughout 9 US states for LTPP. Later, the study processed and analyzed those profiles to get MPD profiles. Those MPD profiles were clustered by using the GMM model, resulting in four distinct groups labeled as fine texture, moderate texture, threshold texture, and peak texture. A medoid-based optimization technique was performed to determine a cluster-specific profile from each group. We performed ordered logistic regression to reveal significant factors contributing to pavement texture. The statistical model correctly classified 58.46% of the clusters, and the moderate results for weighted precision, weighted recall, weighted F1-score, McFadden's, pseudo-$R^2$, Cox & Snell $R^2$, Nagelkerke $R^2$, Log-Likelihood, and Likelihood Ratio Test. However, the important insight from statistical analysis was that eight factors showed high multicollinearity. IRI, AADTT, 18-kip ESAL, precipitation, and temperature were the most critical factors, while different subgrade types and asphalt volumetric properties were mildly influential.

According to statistical results, we performed fourteen different machine learning models with these ten variables, neglecting the multicollinearity issue. WeightedEnsemble_L2 and KNeighborsDist showed better results than other models, having the score_test 0.846154 and valid_test 0.903226. The tree-based algorithms - RandomForestEntr, RandomForestGini, ExtraTreesEntr, ExtraTreesGini – performed promising accuracy of 0.794872. While the boosting-tree algorithm's overall performance was good, non-tree-based models, NeuralNetFastAI and NeuralNetTorch depicted worse predictive performance. The feature importance from machine learning models aligns with domain knowledge and statistical analysis. Precipitation was the most critical variable of all fourteen models, while AADT, 18-kip ESAL, and IRI were also influential factors. The study was an in-depth texture analysis with traffic, weather, aggregate, and volumetric properties, where weather and traffic effects were prominent. The findings could enhance the deeper understanding of pavement surface characteristics and the critical insights about different factors that might help in pavement management.

**Acknowledgement:** The authors would like to express their sincere thanks to Prof. Joshua Li, Kundan Parajulee and Mahtab Delfanazari for their contributions in this research.

## Reference

Guangwei, Yang., Kelvin, C., P., Wang., Joshua, Qiang, Li. (2021). Multiresolution analysis of three-dimensional (3D) surface texture for asphalt pavement friction estimation. International Journal of Pavement Engineering, 22(14):1882-1891. doi: 10.1080/10298436.2020.1726350

Zhen, Leng., Zepeng, Fan., Peng, Liu., J., Kollmann., Markus, Oeser., Dawei, Wang., Xi, Jiang. (2023). Texturing and evaluation of concrete pavement surface: A state-of-the-art review. Journal of road engineering, doi: 10.1016/j.jreng.2023.08.001

Xiangxi, Tian., Yong, Xu., Fulu, Wei., Oguz, Gungor., Zhixin, Li., Ce, Wang., Shuo, Li., Jie, Shan. (2020). Pavement Macrotexture Determination Using Multi-View Smartphone Images. Photogrammetric Engineering and Remote Sensing, 86(10):643-651. doi: 10.14358/PERS.86.10.643

Qiang, Joshua, Li., You, Zhan., Guangwei, Yang., Kelvin, C., P., Wang. (2020). Pavement skid resistance as a function of pavement surface and aggregate texture properties. International Journal of Pavement Engineering, 21(10):1159-1169. doi: 10.1080/10298436.2018.1525489

 doi:10.20944/preprints202603.1280.v1



E. Elkins, Gary, and Barbara Ostrom. 2019. "Long-Term Pavement Performance Information Management System User Guide." FHWA-RD-03-088 (revision). 6300 Georgetown Pike McLean, VA 22101-2296: Federal Highway Administration.

V., Sunitha., Amirthalingam, Veeraragavan., Karthik, K., Srinivasan., Samson, Mathew. (2012). Cluster-Based Pavement Deterioration Models for Low-Volume Rural Roads. International Scholarly Research Notices, 2012:1-8. doi: 10.5402/2012/565948

C., Plati., M., Pomoni., T., Stergiou. (2019). From Mean Texture Depth to Mean Profile Depth: Exploring possibilities. 660-665. doi: 10.1201/9781351063265-86

Sachin, Gowda., C., S., Nandan., M.A., Jayaram., Aakash, Gupta., Rachman, Jaya. (2023). Unsupervised Clustering of Asphalt Pavement Conditions Using Fuzzy C-Means Algorithm with Principal Component Analysis Aided Dimensionality Reduction. 35-45. doi: 10.1007/978-981-99-8135-9_4

DanWang., ZaijunZhang., JinchengZhou., BenfeiZhang. (2022). Comparison and Analysis of Several Clustering Algorithms for Pavement Crack Segmentation Guided by Computational Intelligence. Computational Intelligence and Neuroscience, 2022:1-13. doi: 10.1155/2022/8965842

Li, Q., Wang, K., Eacker, M., & Zhang, Z. (2017). Clustering Methods for Truck Traffic Characterization in Pavement ME Design. ASCE-ASME Journal of Risk and Uncertainty in Engineering Systems, Part A: Civil Engineering, 3. https://doi.org/10.1061/AJRUA6.0000881.

Mukhtarli, K. (2020). Machine learning for homogeneous grouping of pavements.

Sampaio, R., Garcia, J., Poggi, M., & Vidal, T. (2023). Regularization and optimization in model-based clustering. Pattern Recognit., 150, 110310. https://doi.org/10.1016/j.patcog.2024.110310.

Zhao, Y., Shrivastava, A., & Tsui, K. (2019). Regularized Gaussian Mixture Model for High-Dimensional Clustering. IEEE Transactions on Cybernetics, 49, 3677-3688. https://doi.org/10.1109/TCYB.2018.2846404.

Mohammad, D., & Ismael, M. (2021). Evaluating the Friction Characteristics of Pavement Surface for Major Arterial Road. Civil Engineering Journal. https://doi.org/10.28991/cej-2021-03091775.

Ozdemir, D., Topal, A., Kaçmaz, B., & Sengoz, B. (2021). Evaluating the asphalt pavement's surface characteristics by field testing. . https://doi.org/10.7764/RDLC.19.3.474-485.

Edmondson, V., Martin, J., Ardill, O., Lim, M., Kane, M., & Woodward, J. (2021). Seasonal Signals Observed in Non-Contact Long-Term Road Texture Measurements. Coatings. https://doi.org/10.3390/coatings11060735.

Kodippily, S., Yeaman, J., Henning, T., & Tighe, S. (2018). Effects of extreme climatic conditions on pavement response. Road Materials and Pavement Design, 21, 1413 - 1425. https://doi.org/10.1080/14680629.2018.1552620.

Wu, X., Zheng, N., & Kong, F. (2020). The analysis of the factors affecting the macrotexture of bauxite clinker aggregate gradation. Construction and Building Materials. https://doi.org/10.1016/j.conbuildmat.2020.118334.

Praticò, F., & Briante, P. (2020). Prediction of surface texture for better performance of friction courses. Construction and Building Materials, 230, 116991. https://doi.org/10.1016/j.conbuildmat.2019.116991.

Chen, H., Wang, R., & Bahia, H. (2023). Effect of air voids on the fracture resistance of HMA in the indirect tensile cracking (IDEAL-CT) test. International Journal of Pavement Engineering, 24. https://doi.org/10.1080/10298436.2023.2252148.

John, I., Bangi, M., & Lawrence, M. (2021). Effect of Filler and Binder Contents on Air Voids in Hot-Mix Asphalt for Road Pavement Construction. Open Journal of Civil Engineering. https://doi.org/10.4236/ojce.2021.113016.

Slebi-Acevedo, C., Pascual-Muñoz, P., Lastra-González, P., & Castro-Fresno, D. (2019). Multi-Response Optimization of Porous Asphalt Mixtures Reinforced with Aramid and Polyolefin Fibers Employing the CRITIC-TOPSIS Based on Taguchi Methodology. Materials, 12. https://doi.org/10.3390/ma12223789.

Munna, M. R., Chatterjee, K., & Li, J. Q. (2025). Evaluating Pavement Surface Texture with LTPP Database. *International Journal of Pavement Research and Technology*, 1-14.

Rana Munna, M., Chatterjee, K., Parajulee, K., & Li, J. Q. Effect of Pavement Surface Characteristics on Adverse Road Conditions. In *Airfield and Highway Pavements 2025* (pp. 360-369).

Chatterjee, K., Li, J. Q., Ansari, F., Munna, M. R., Parajulee, K., & Schwennesen, J. (2026a). Hybrid LSTM-Transformer Models for Profiling Highway–Railway Grade Crossings. *Journal of Transportation Engineering, Part A: Systems*, *152*(2), 04025138.

Chatterjee, K., Desai, M., & Li, J. (2026b). Application of Large Language Models in Geotechnical Engineering: A Movement Towards Safe and Sustainable Future.

 doi:10.20944/preprints202603.1280.v1



Desai, M., & Chatterjee, K. (2026). Application of Machine Learning Techniques for Prediction of Soil Water Characteristics Curve: A State of the Art Review.

Chatterjee, K., Vivanco, D., Yang, X., & Li, J. Q. (2024). Enhancing pavement performance through balanced mix design: A comprehensive field study in Oklahoma. In *International Conference on Transportation and Development 2024* (pp. 511-522).

Bashar, M., & Torres-Machí, C. (2021). Performance of Machine Learning Algorithms in Predicting the Pavement International Roughness Index. Transportation Research Record, 2675, 226 - 237. https://doi.org/10.1177/0361198120986171.

Naseri, H., Jahanbakhsh, H., Foomajd, A., Galustanian, N., Karimi, M., & Waygood, E. (2022). A newly developed hybrid method on pavement maintenance and rehabilitation optimization applying Whale Optimization Algorithm and random forest regression. International Journal of Pavement Engineering, 24. https://doi.org/10.1080/10298436.2022.2147672.

Abdualmtalab, A., Ali[1], A., & Milad, A. (2023). Application of Machine Learning Techniques for Asphalt Pavement Performance Prediction. Journal of Pure & Applied Sciences. https://doi.org/10.51984/jopas.v22i3.2733.

Hoang, N. (2019). Automatic detection of asphalt pavement raveling using image texture-based feature extraction and stochastic gradient descent logistic regression. Automation in Construction. https://doi.org/10.1016/J.AUTCON.2019.102843.

J.N. Meegoda, G.M. Rowe, C.H. Hettiarachchi, N. Bandara, M.J. Sharrock, Correlation of Surface Texture, Segregation, and Measurement of Air Voids, FHWA-NJ-2002-026, Federal Highway Administration U.S. Department of Transportation, Washington, D.C., 2002.

Williams, R. (2016). Understanding and interpreting generalized ordered logit models. The Journal of Mathematical Sociology, 7-20.

Kim, J. H. (2019). Multicollinearity and misleading statistical results. Korean Journal of Anesthesiology, 558-569.

Géron, A. (2019). Hands-on machine learning with scikit-learn, keras, and tensorflow: concepts. *Aurélien Géron-Google Kitaplar, yy https://books. google. com. tr/books*.

Breiman, L. (2001). Random forests. Machine Learning, 45(1), 5–32.

Geurts, P., Ernst, D., & Wehenkel, L. (2006). Extremely randomized trees. Machine Learning, 63(1), 3–42. https://doi.org/10.1007/s10994-006-6226-1

Si, S., Zhang, H., Keerthi, S. S., Mahajan, D., Dhillon, I. S., & Hsieh, C. J. (2017). Gradient boosted decision trees for high dimensional sparse output. 34th International Conference on Machine Learning, ICML 2017, 7, 4899–4908.

Machado, M. R., Karray, S., & De Sousa, I. T. (2019). LightGBM: An effective decision tree gradient boosting method to predict customer loyalty in the finance industry. 14th International Conference on Computer Science and Education, ICCSE 2019, Nips, 1111–1116. https://doi.org/10.1109/ICCSE.2019.8845529

Liu, M.Y. & Jiang, Y.B. (2021). Review of neural network algorithms. In Proceedings of The International Conference on Electronic Business, Volume 21 (pp. 392-401). ICEB'21, Nanjing, China, December 3-7, 2021.

Alzubaidi, L., Zhang, J., Humaidi, A. J., Al-Dujaili, A., Duan, Y., Al-Shamma, O., Santamaría, J., Fadhel, M. A., Al-Amidie, M., & Farhan, L. (2021). Review of deep learning: concepts, CNN architectures, challenges, applications, future directions. In Journal of Big Data (Vol. 8, Issue 1). Springer International Publishing. https://doi.org/10.1186/s40537-021-00444-8

Qi, W., Xu, C., & Xu, X. (2021). AutoGluon: A revolutionary framework for landslide hazard analysis. Natural Hazards Research, 1(3), 103–108. https://doi.org/10.1016/j.nhres.2021.07.002

Erickson, N., Mueller, J., Shirkov, A., Zhang, H., Larroy, P., Li, M., & Smola, A. (2020). AutoGluon-Tabular: Robust and Accurate AutoML for Structured Data. http://arxiv.org/abs/2003.06505